SMART-PHONE-BASED ELECTROCHEMICAL SENSOR FOR ENVIRONMENTAL APPLICATIONS

BY

XINHAO WANG

THESIS

Submitted in partial fulfillment of the requirements
for the degree of Master of Science in Electrical and Computer Engineering
in the Graduate College of the
University of Illinois at Urbana-Champaign, 2015

Urbana, Illinois

Adviser:

Associate Professor Gang Logan Liu

ABSTRACT

We demonstrated a mobile phone sensing platform, MoboSens, with integrated plug-n-play microelectronic ionic sensor that performs electrochemical measurement by using audio jack of a smart phone. This platform was used to measure nitrate concentration using a few microliter liquid samples on field along with providing geospatial map locations through a wireless network. This compact MoboSens platform (~65 gram), based on a smart phone, is able to detect nitrate concentration in water with a detection limit of 0.2 ppm within 1 minute. The nitrate ion detection on MoboSens platform is performed by a microfabricated microfluidic sensor utilizing a cyclic voltammetry based electrochemical process. The stability of the measurements was verified by performing the experiments under varying temperature, pH and ion interference conditions. The mobile phone app reports the quantitative nitrate sensing results along with user-input metadata. The results can be automatically saved on secure cloud servers or can be pushed on public social media, e.g., Twitter. Finally, the digital sensing information can be retrieved with geospatial information tagged on an internet map service, e.g., Bing Map, for public sharing and viewing. We tested this lab-on-a-chip mobile sensing platform for field water quality measurement and confirmed our mobile sensing results with other existing analytical testing methods.

To my parents, for their love and support

ACKNOWLEDGMENTS

I would like to first deliver my sincere gratitude to my master's and PhD adviser, Professor Gang Logan Liu, for his helpful guidance and advice, and especially for giving me this opportunity to pursue my degree and conduct research at the University of Illinois at Urbana-Champaign. I would like to thank all the group members in the Liu Nanobionics Laboratory, particularly Manas Ranjan Gartia, Te-Wei Chang, Jing Jiang, Zidar Xu and Sujin Seo, for their indispensable help and discussions. I would like to thank the staff of the Micro and Nanotechnology Laboratory and Materials Research Laboratory for their technical support. Finally I thank my families and friends, especially my girlfriend Lynne Meng, who gave me comfort and support.

TABLE OF CONTENTS

CHAPTER 1

INTRODUCTION

1.1 Electrochemistry and cyclic voltammetry

Electrochemistry is the branch of chemistry concerned with the combination of electrical and chemical effects. The electrochemical method has been developed for hundreds of years. With the development of nanotechnology, more sensitive and accurate micro- or nano-electrodes have been designed and fabricated, bringing the electrochemical method back to the platform for point-of-care testing. With the development of microfluidic systems, integration of chemical or biological sensing can be achieved by making use of the electrochemical method.

Compared with some classic analytical chemical detection methods, like high performance liquid chromatography (HPLC) or enzyme-linked immunosorbent assay (ELISA), the advantage of the electrochemical method is its portability, convenience and integration potential to electronic devices.

Cyclic voltammetry or CV is a type of potentiodynamic electrochemical measurement. In a cyclic voltammetry experiment the working electrode potential is ramped linearly versus time. Unlike in linear sweep voltammetry, after the set potential is reached in a CV experiment, the working electrode's potential is ramped in the opposite direction to return to the initial potential. These cycles of ramps in potential may be repeated as many times as desired. The current at the working electrode is plotted versus the applied voltage (i.e., the working electrode's potential) to give the cyclic voltammogram trace. Cyclic voltammetry is generally used to study the electrochemical properties of an analyte in solution [1, 2, 3].

For an electrochemical system with only oxide in solution, the governing equation for single-side linear voltage sweeping is [1]:

$$\mathrm{E} = E^{0'} + \frac{RT}{nF} ln \frac{C_O(0,t)}{C_R(0,t)} \tag{1.1}$$

$$\mathrm{E(t)} = E_i - vt \tag{1.2}$$

$$-J_O(0,t) = \frac{i(t)}{nFA} = D_O \left[\frac{\partial C_O(x,t)}{\partial x}\right] \ (x = 0) \tag{1.3}$$

$$\frac{\partial C_O(x,t)}{\partial t} = D_O \frac{\partial^2 C_O(x,t)}{\partial x^2} \tag{1.4}$$

$$\frac{\partial C_R(x,t)}{\partial t} = D_R \frac{\partial^2 C_R(x,t)}{\partial x^2} \tag{1.5}$$

At the interface of metal electrode and solution, the boundary equations are [1]:

$$C_O(x,0) = C_O^* \tag{1.6}$$

$$\lim_{x\to\infty} C_O(x,t) = C_O^* \tag{1.7}$$

$$C_R(x,0) = 0 \tag{1.8}$$

$$\lim_{x\to\infty} C_R(x,t) = 0 \tag{1.9}$$

$$D_O(\frac{\partial C_O(x,t)}{\partial x})_{x=0} + D_R(\frac{\partial C_R(x,t)}{\partial x})_{x=0} = 0 \tag{1.10}$$

By solving the above equations and boundary conditions, the peak current intensity can be written as [1]:

$$i_p = (2.69 \times 10^5) n^{3/2} A D_O^{1/2} C_O^* v^{1/2} \tag{1.11}$$

The current density is linearly proportional to the concentration of analyte at the fixed voltage sweeping rate. Figure 1.1 shows the diffusion and electron transfer process near the electrode surface and the corresponding cyclic voltammetry curve showing the reduction peak current.

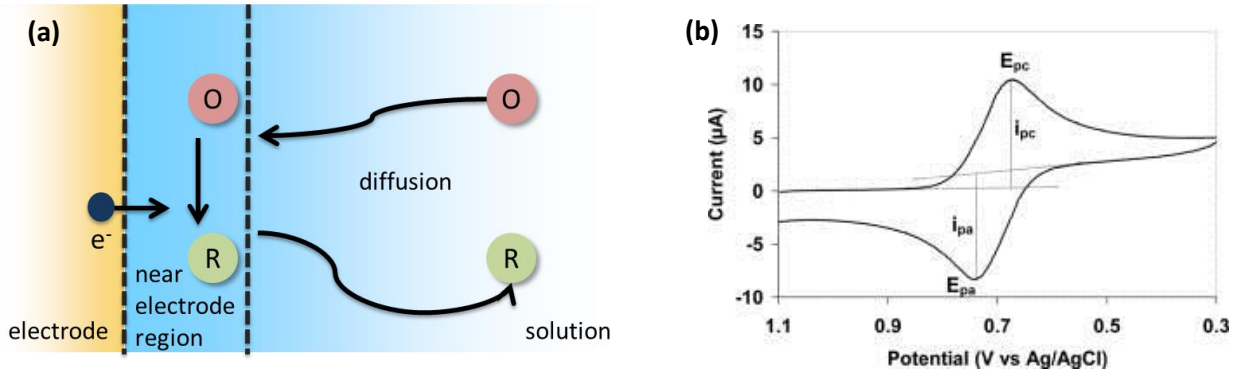

Figure 1.1 (a) Diffusion and electron transfer near the electrode surface. **(b)** Cyclic voltammetry curve with current at y axis and potential at x axis.

1.2 Three-electrode system

The traditional electrochemical testing system was based on two electrodes: the working electrode and reference electrode. The working electrode is where electrochemical reaction occurs with electron transfer. The material for the working electrode is normally chosen to be sensitive to redox target. The reference electrode provides stable potential with the passage of current over time. There are some standard reference electrodes like normal hydrogen electrode (NHE), saturated calomel electrode (SCE) and silver-silver chloride electrode. There are some drawbacks to this kind of two-electrode system. The passage of current through the reference electrode over time will depolarize it, inducing drift in the stable potential. This small voltage drift between the working and reference electrodes may cause large inaccuracy in measurement, so a three-electrode system is used nowadays by adding a counter electrode which can help pass most of the current to ensure the stable potential of the reference electrode. The material for the

counter electrode is often chosen to be gold or platinum, which are not easy to polarize. And the size of counter electrode is normally the largest, which can assist the conduction of current.

1.3 Electrolyte

The electrolyte could be a kind of salt solution which contains a large amount of non-reactive ions and can help with the adjustment of the pH value. Before talking about the functionality of the electrolyte, we introduce the three modes of possible mass transfer inside a solution. Movement of a charged body under the influence of an electric filed is defined as migration, which can be a main interfering factor for the measured current in an electrochemical system. Movement of a species under the influence of a gradient of chemical potential is defined as diffusion, which reflects the concentration gradient. The stirring or hydrodynamic transport is defined as convection, which is seldom used in electrochemical modeling. Because of the concentration gradient, diffusion is often used to quantify the concentration of target reactive ions; the effect of migration should be eliminated as much as possible. The existence of electrolyte could help eliminate the current contribution from migration with much higher concentration than the target reactive ions. The existence of electrolyte can also help to adjust the pH environment, which is very critical to some electrochemical reactions.

1.4 Miniaturized electrode

Micro- or nano-electrodes have been developed in recent years for quicker and more accurate sensing by achieving smaller time constants and lower ohmic drops. Because of the small distance between the working and reference electrodes, the resistance (uncompensated resistance) between these two electrodes will be much smaller. Since the time constant is the product of uncompensated resistance and double layer capacitance, this small time constant guarantees the

quick response to potential steps. Another advantage of miniaturized electrodes is the easy fabrication process which can be simply achieved by integrated circuit fabrication techniques.

CHAPTER 2

MINIATURIZED THREE-ELECTRODE SYSTEM FOR NITRATE REDUCTION

2.1 Overview

Even though nitrogen is a vital part of living organisms, as a component of amino acids, proteins and nucleic acids (DNA), excessive nitrogen has adverse health and environmental impacts [1]. In the US, EPA (Environmental Protection Association) regulates the maximum allowable contamination level for nitrate as nitrogen (NO_3-N) to be 10 ppm (10 mg/L) so as to prevent adverse health effects on population [2]. Nitrite (NO_2-), a reduced form of nitrate, is also a major cause of poisoning in fish and is toxic to human health as well. Therefore, the effective and accurate detection of nitrate concentration has become significant and necessary.

Currently citizens are not equipped to detect invisible contaminants in water as it requires specialized instruments, a certain level of expertise and costly equipment and chemicals for measurement. In addition to the general public, people such as environmentalists, tourists and farm owners may often need to determine water contamination, so an easy-to-operate, low-cost and portable platform for nitrate detection is an unmet need. Moreover, a nitrate sensor operated by a mobile phone platform will be quite helpful in achieving mapped information about contaminants, since such information comes with location and temperature information. Also, these data can be sent to social platforms normally connected to cloud server for wider dissemination.

Many existing methods such as spectroscopy, chromatography, capillary electrophoresis and electrochemistry are available to determine nitrate concentration [3]. Spectroscopy is broadly

used for nitrate determination, mainly using UV/Vis or fluorimetric emission [4]. This method normally involves the use of chemical reactions like Griess reaction to form highly fluorescent compounds to be compared and measured using a spectrophotometer [5, 6, 7]. The detection limit achievable by this method is in between 0.28 ppb and 28 ppb [3]. But multiple reaction steps make this method time-consuming; also the instrument for fluorescence spectroscopic detection is not accessible to common citizens. Gas chromatography and ion chromatography are also commonly used in laboratory set-ups [8, 9, 10, 11]. Although the process is accurate, some experiment requirements like high pressure for HPLC (high-pressure liquid chromatography) and long column (200 mm) [9] make it difficult to miniaturize. The flow rate control of the mobile phase is also sensitive to vibration or trembling and hence unsuitable for a portable device. Further, due to the associated high cost and large form factor, it is unlikely to be adopted by regular citizens for routine nitrate measurements. For capillary electrophoresis, the column used is even longer and the set-up for fluorescence detection is complicated [12, 13].

Compared with other methods, electrochemistry is relatively easy to operate and can be transformed to a portable platform [3]. In electrochemical methods, due to the application of voltage potential between reference and working electrodes, oxidation or reduction of electro-active species happens [14]. Cyclic voltammetry is a popular method often used in electrochemistry systems [1, 15, 16] because of its ease of data interpretation. Miniaturized or microscale electrodes along with microfluidic integration greatly reduce the required liquid sample volume and will make the whole package portable [17].

2.2 Design of miniaturized three electrodes

Due to the advantages mentioned in the last chapter, a miniaturized three-electrode system was developed for cyclic voltammetry testing. The electrodes are designed in a circular fashion to

enable uniformity in the current flow in the electrochemical system. The surface area of the counter, working and reference electrode are $9.05\times10^{-4}cm^2$, $7.05\times10^{-4}cm^2$ and $3.47\times10^{-4}cm^2$ respectively. The area of counter electrode is designed to be the largest for preventing oxygen-bubble formation on its surface due to OH^- oxidation at high current density [18]. The design and fabrication process are illustrated in Figure 2.1. In order to minimize uncompensated resistance (R_u) between reference and working electrodes, these two electrodes are kept close to each other (10 μm) to increase accuracy. As an advantage of miniaturized electrodes, this will directly result in much smaller cell time constant, which is the product of R_u and double-layer capacitance (C_d). Smaller cell time constant leads to a lower limit of the experimental time scale.

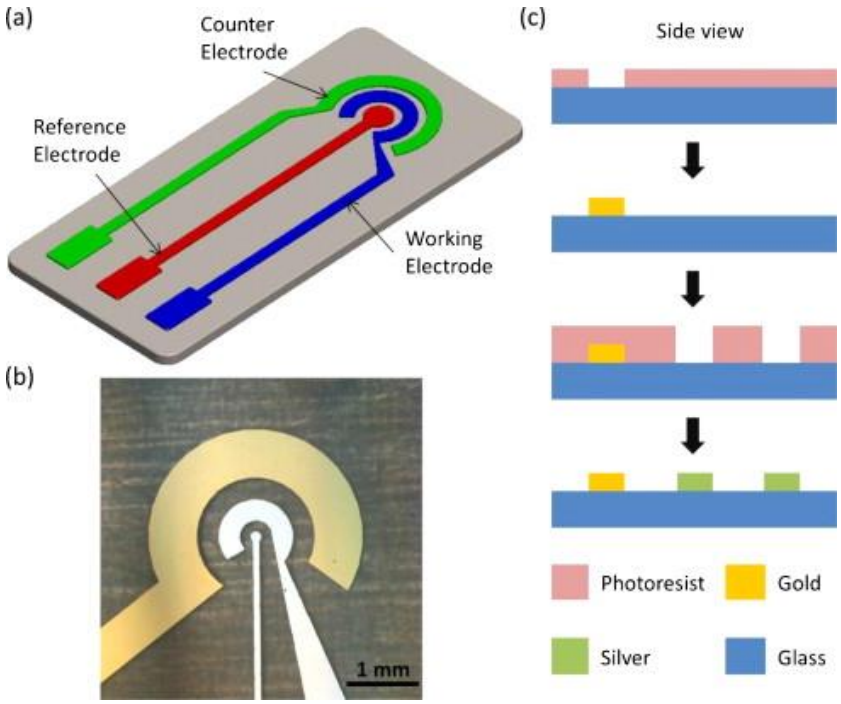

Figure 2.1 Sensor electrodes and fabrication process. **(a)** Schematic showing the three-electrode electrochemical sensor utilized in the MoboSens. **(b)** Optical image of the fabricated sensor electrodes. **(c)** Schematic showing the fabrication process involving series of photolithography and lift-off to fabricate the electrochemical miniaturized sensor.

2.3 Material and electrolyte chosen for three-electrode system

The target nitrate concentration we are interested will not exceed 10mM, so the concentration of electrolyte was chosen to be 0.1M which is at least 10 times higher than the target ion concentration. Ag/AgCl is usually used as reference electrode, but it may also provide chloride contamination during nitrate detection. Instead, silver is used as reference electrode due to its simplicity in fabrication and sufficient stable potential in 0.1 M NaOH electrolyte [18, 19]. It has been reported that silver has high sensitivity for reducing nitrate ions in alkaline environment [20, 21]. Although copper electrode also shows this good property in acidic solution [22, 23], it was found to dissolve during the reduction of nitrate [22]. That is why we chose silver as the working electrode here. For better conductivity and stability, gold was chosen for the counter electrode.

2.4 Fabrication process of three electrodes

The schematic of fabrication process is in Figure 2.1. We first patterned the counter electrode by optical lithography and deposited 200 nm gold by electron beam (e-beam) evaporation. After lifting off with acetone, the gold inside counter electrode region will be left. With the same method, another layer of silver (200 nm) is fabricated as reference and working electrodes. For better adhesion on glass, one layer of titanium (20 nm) instead of chromium was deposited before gold and silver evaporation because the chromium adhesion layer severely corrodes during the electrochemical activation process [18].

2.5 Cyclic voltammetry experiment

Cyclic voltammetry method is used to obtain the reduction/oxidation reaction in the electrochemical system. The voltage sweeping range available for MoboSens is -1.6V~+1.5V. Sodium hydroxide (NaOH) is used as electrolyte and sodium nitrate with different concentrations is added to the electrolyte for testing. The concentration of electrolyte (NaOH) is made to be 100

mM to eliminate the contribution of migration to the mass transfer of electroactive species. The potential of hydrogen evolution will also be pushed to a more negative value in such an alkaline environment [24]. The electrodes are first activated by sweeping the potential from -1.5 V to 1.0 V for 20 cycles (scan rate 1 V/s) with final potential at -1.5V. This activation process will remove the possible oxidation layer at the surface of the working electrode [25, 26, 27]. In order to avoid oxidation of silver working electrode and to make nitrate reduction happen, the sweeping voltage between working and reference electrodes is chosen from 0 V to -1.5 V with a sweeping rate of 100 mV/s for cyclic voltammetry testing. This sweeping rate guarantees only 30 seconds for one cycle measurement without severe distortion which normally occurs at high sweeping rate due to extra charging current from double-layer capacitance. We start sweeping from the cathode because the reverse process is always less precise by referencing forward, which is uncertain in folded faradaic response [19]. The reduction peak of the nitrate will be detected when sweeping toward -1.5 V. The whole test involved 4 cycles and the data from the fourth cycle was used for calculation as the reduction peaks were stabilized in roughly 3 cycles.

2.6 Miniaturized nitrate sensor characterization

Nitrate reduction in alkaline media is either a two-electron (94%) or eight-electron (6%) process as given below:

$$NO_3^- + H_2O + 2e^- \rightarrow NO_2^- + 2OH^- \text{ [16]} \quad (2.1)$$

$$NO_3^- + 6H_2O + 8e^- \rightarrow NH_3 + 9OH^- \text{ [15, 16]} \quad (2.2)$$

Standard testing samples with different nitrate concentrations from 100 μM (1.4 ppm NO_3-N) to 4000 μM (64 ppm NO_3-N) were first measured by a commercial potentiostat (CHI600) with a sweeping rate of 100 mV/s. The reduction current peaks were found around -1.35 V in Figure 2.2

(a), which shows a linear relationship with concentration. The fact that the peak potential is more negative than in previous experiments from other research groups [15, 16, 25, 28] can be attributed to the more positive standard reduction potential of the reference electrode. This current peak is caused by the reduction of nitrate since the peak value increases with the increase of nitrate concentration. Since we used silver (Ag/Ag+) as our reference electrode which acts as a pseudo reference electrode (not ideally nonpolarizable electrode), it showed a modest drift (about 20mV) at higher concentration of nitrate [18]. In order to quantify the effect of interference on nitrate detection due to common soluble anions like chloride, carbonate, sulfate and phosphate, the interfering ionic solution was mixed with the nitrate standard solution. Nitrate standard solution with a concentration of 250 μM was mixed with chloride, carbonate, sulfate and phosphate at the same concentration respectively. Figure 2.2 (b) shows the similar location (-1.4V ~ -1.38V) for nitrate reduction peak, with a coefficient of variation (COV) of only 0.4%, which means the measurement is not interfered much by those interference ions. The COV is calculated by taking the ratio of standard deviation and the mean value. We found that the COV for the magnitude of reduction peak current is only 1.7%, which indicates the accuracy of the sensor for measuring nitrate. This indicates the material of the working electrode (Ag) and the strongly alkaline environment shows higher selectivity to nitrate reduction.

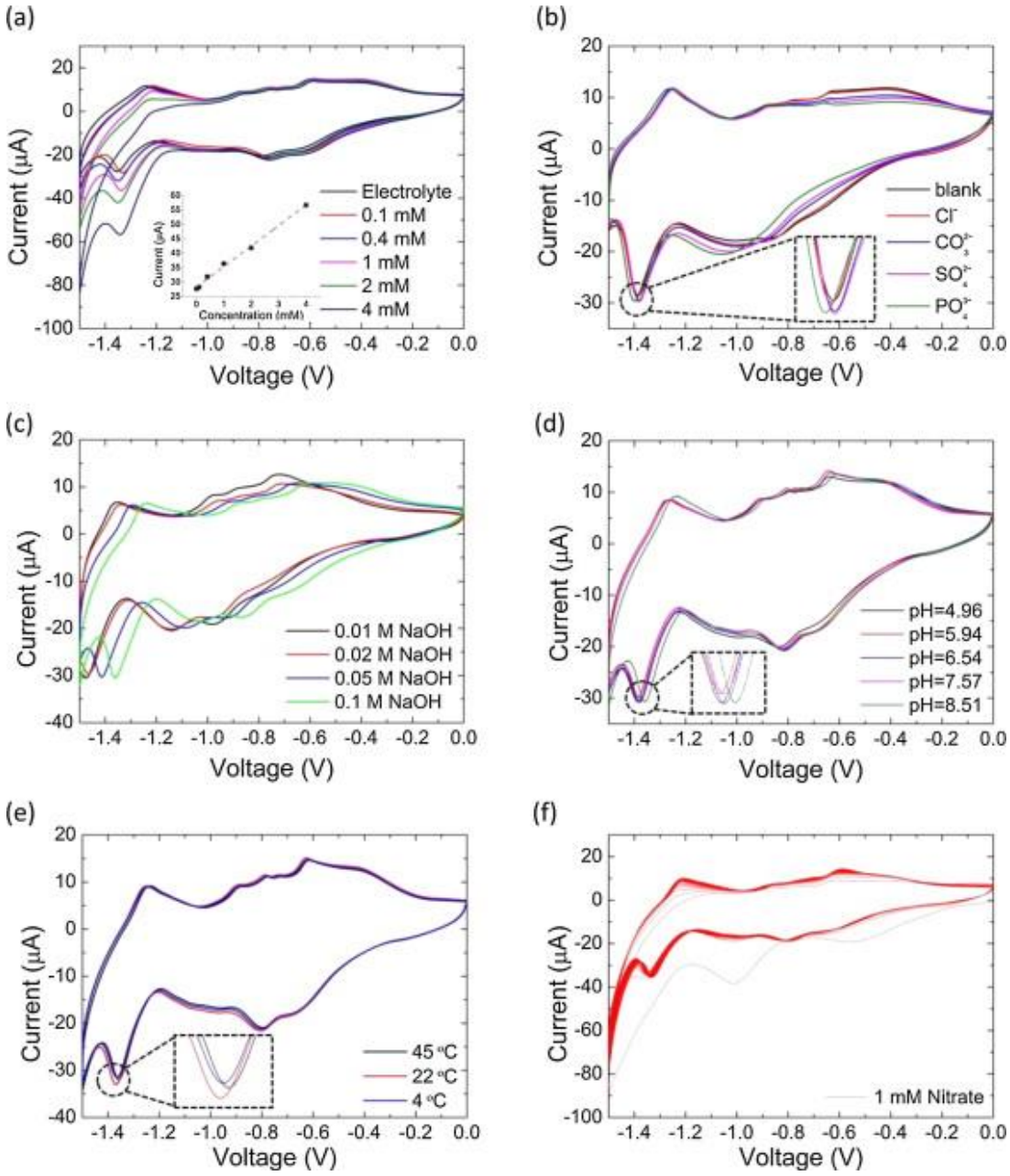

Figure 2.2 Characterization of miniaturized sensor. **(a)** Raw data and calibration curve of standard nitrate solution (0.1 mM ~ 4 mM) using commercial potentiostat. The electrolyte (NaOH) concentration is 100 mM. **(b)** Effect of interfering ions: separate tests were performed by mixing NaCl (0.25 mM), Na2CO3 (0.25 mM), Na2SO4 (0.25 mM) and Na3PO4 (0.25 mM) solution to nitrate standard solution of 0.25 mM. The electrolyte (NaOH) concentration is 100 mM. **(c)** Effect of electrolyte concentration: cyclic voltammetry for 1 mM nitrate standard solution at different electrolyte (NaOH) concentrations (pH value: 12 ~ 13). **(d)** Effect of pH of the test solution: cyclic voltammetry for 1 mM nitrate standard solution at simulated soil water pH environment showing little effect of solution pH on the reduction peak position. The electrolyte (NaOH) concentration is 100 mM. **(e)** Effect of temperature of the solution: 1 mM standard nitrate solution was tested under different temperatures with 100 mM electrolyte (NaOH). **(f)** Stability of sensor: cyclic voltammetry testing was performed 100 times. The sweeping rate for cyclic voltammetry method above is 100 mV/s.

The effect of electrolyte concentration was characterized by mixing a nitrate standard solution of the same concentration as the sodium hydroxide solution at different concentrations. In Figure 2.2 (c), the positions of the nitrate reduction current peak shifts from -1.35V to -1.45V with decreasing concentration of sodium hydroxide from 0.1M to 0.01M. The main reason for this shift could be the increase of uncompensated resistance (R_u) between working and reference electrodes as the electrolyte concentration is decreased by ten times [19]. So we keep the electrolyte concentration at 0.1M to keep the reduction peak away from the sweep turning point (-1.5 V) for accuracy. Different pH values may also have some effect on the potential shift. Since the nitrate reduction process is irreversible [24], the peak potential E_p, where the peak current is, can be expressed in theory as:

$$E_p = E^{0\prime} - \frac{RT}{\alpha F}\left[0.780 + \ln\left(\frac{D_O^{1/2}}{k^0}\right) + \ln\left(\frac{\alpha F v}{RT}\right)^{1/2}\right] \text{[19]} \qquad (2.3)$$

$E^{0\prime}$ is the formal potential of an electrode; R is gas constant; T is temperature; F is the Faraday constant; α is transfer coefficient; v is voltage sweeping rate; D_O is diffusion coefficient of oxidant; k^0 is the standard heterogeneous rate constant. It has been reported that the diffusion coefficient will increase with the decrease of pH value of the solution, especially with significant slope at low and high pH environment [29]. This can help explain the negative shift of peak potential shown in our experiments.

A further experiment was implemented to simulate the effect on soil water at different pH levels. Standard pH solutions containing the same amount of nitrate varying from “very strong acid” (pH: 4.5 ~ 5.0) to “strongly alkaline” (pH: 8.5 ~ 9.0) [30] were dragged separately into a micro-fluid chamber where sodium hydroxide solution at 0.1 M was pre-dried inside. Figure 2.2 (d)

shows about 30 mV positive shift of peak potential as the pH value increases, which indicates a wide coverage of the MoboSens platform for soil water at different pH levels.

The temperature effect was also determined by adding nitrate solution at 1mM from the environment at 45 ℃, 22 ℃ and 4 ℃ respectively in Figure 2.2 (e). The coefficient of variation (COV) is within 2%, which indicates that temperature has little effect on the nitrate reduction current peak position.

Finally, repeatability of the miniaturized electrode was characterized by running cyclic voltammetry 100 times in nitrate solution at 1 mM in Figure 2.2 (f). The nitrate reduction peak current began to stabilize after the 4th cycle. By analyzing data from the 5th, 40th and 80th cycle, the COV was found to be 1.5%, which indicates this platform could be used for repeatable testing.

CHAPTER 3

SENSOR INTEGRATION TO SMART PHONE THROUGH AUDIO JACK

3.1 Overview

The schematic model of MoboSens is shown in Figure 3.1 (a) and (b). A photograph of the complete package of MoboSens including the microfluidics, mobile apps and the controlling circuits is shown in Figure 3.1 (c). Due to its uniformity in design and availability in all mobile phones, we decided to use the audio jack for the electrical signal input and output of the MoboSens system (instead of the USB port). Figure 3.2 shows the component-level description of the MoboSens system. The sequence of events during the detection of nitrate using MoboSens is as follows: the sweep voltage required for driving the nitrate electrochemical sensor is first generated by the speaker D/A module in the mobile phone. The output voltage from the sensor is simultaneously retrieved by the A/D module embedded in microphone. In order to achieve frequency match between mobile phone and nitrate sensor, a circuit board with modulation and demodulation components is added to the MoboSens system.

A mobile-phone-based software platform is developed to drive and retrieve the data from the nitrate sensor. There is an option to perform real-time calibration or to use a stored calibration curve for the nitrate measurements. The calibration measurements are performed using standard nitrate solutions with different concentrations. Finally, after measurements of the nitrate concentration of field water samples, the results can be shared (on social network like Twitter) or stored in a remote server (for example, cloud server) for further analysis along with the

information about geographical location (latitude and longitude), temperature and user inputs (meta data). The schematic of the entire system is shown in Figure 3.2.

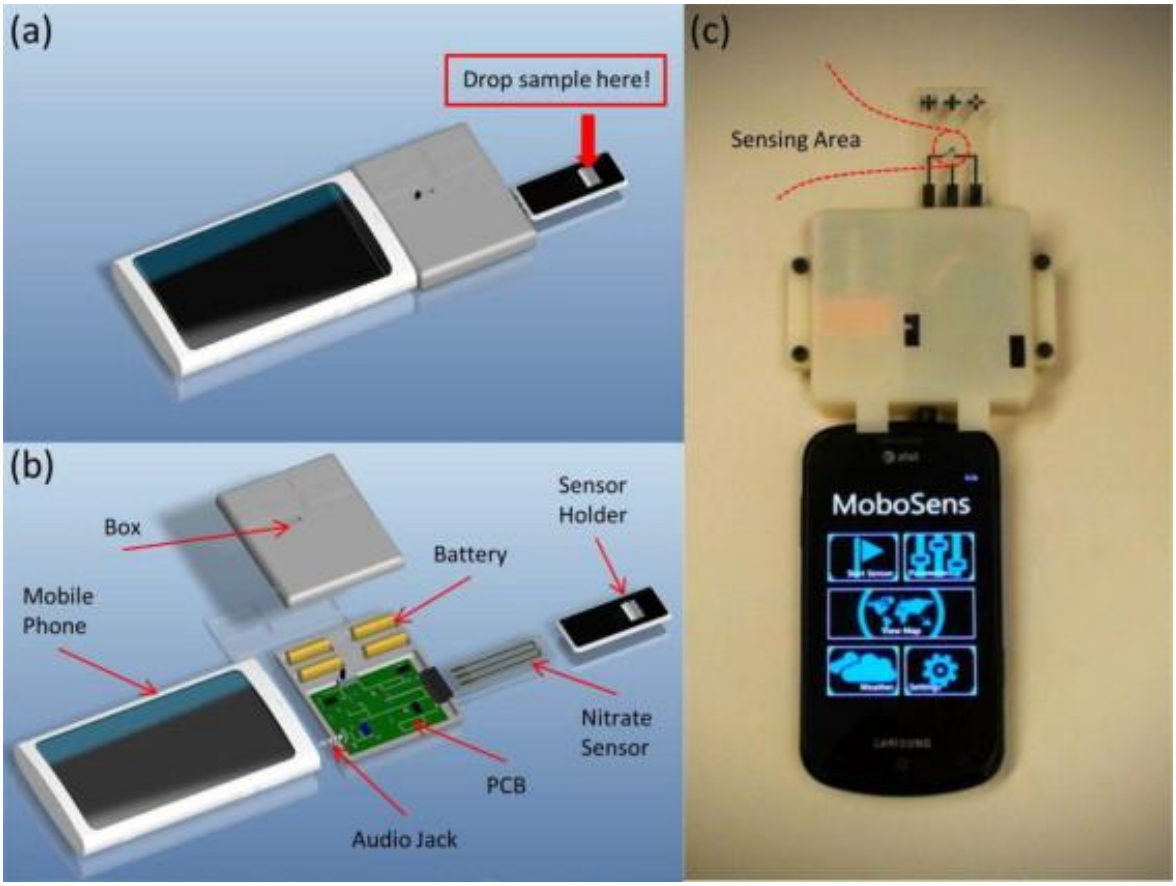

Figure 3.1 Concept design and real package of MoboSens. **(a)** Assembly view of MoboSens. **(b)** Detailed components of MoboSens. **(c)** Photograph showing the complete MoboSens system.

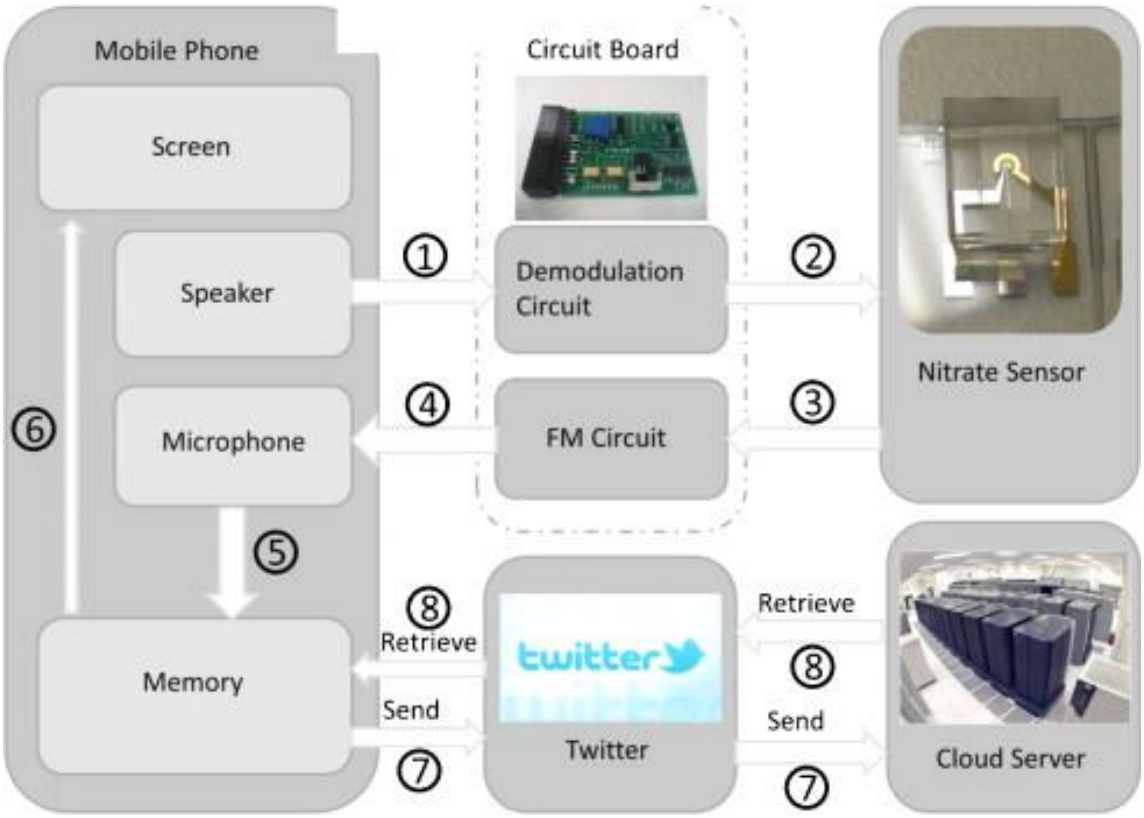

Figure 3.2 Schematic of operation of MoboSens system. **(1)** Signal with changing frequency is generated from speaker to demodulation unit. **(2)** Signal was demodulated to sweeping voltage for cyclic voltammetry testing. **(3)** The output current from miniaturized sensor was transformed to voltage and sent to frequency modulation unit. **(4)** Output signal from sensor was modulated to send to microphone. **(5)** "Recorded" raw data was transformed to frequency and analyzed in memory. **(6)** Frequency vs. time plot was shown on mobile screen. **(7)** Analyzed results were sent to social platform (like Twitter) and stored by cloud server. **(8)** Information from cloud server or social platform could also be retrieved to smart phone for analysis.

3.2 Limitation of audio jack on smart phone

The limitation of the audio jack could be from both the signal generating and signal receiving parts. In the signal generating part, the maximum peak-to-peak voltage of a sine wave function is about 1V and the frequency range is from 20 Hz to 20k Hz. In the signal receiving part, the

maximum peak-to-peak voltage of a sine wave function without truncation is only 200mV and the frequency limit for receiving signal is from 20 Hz to 10k Hz. Since the sweeping voltage for running cyclic voltammetry testing is almost like DC voltage with a frequency as low as 0.033 Hz, a modulation method has to be used to generate this signal. Because of the limitation of peak-to-peak voltage at the signal receiving end, only frequency modulation could be used. Although both amplitude and frequency demodulation could be used to generate the sweeping voltage for cyclic voltammetry testing, frequency demodulation was finally used to break the limitation of different kinds of smart phones (the amplitude varies with different smart phones).

3.3 Circuit design for sensor integration

Since there is a frequency limitation (which must be greater than 20 Hz) for input and output signals from both mobile phone audio jack and microphone, a sine wave at constant amplitude with frequency increasing from 5300 Hz to 7600 Hz and decreasing from 7600 Hz to 5300 Hz is generated from mobile phone audio jack. 5300 Hz corresponds to 0 V while 7600 Hz corresponds to -1.5 V. A frequency demodulation module is added to the circuit to convert frequency to voltage for sweeping voltage detection. This frequency demodulation mechanism enables MoboSens to break through the limitations of different types of smart phones without considering the different speaker volume settings. Since it is common to have some drift within FM chips and resistors, a variation of the order of 25 mV is expected when converting frequency values to voltages. The cyclic sweeping voltage is then added to the reference potential and the working electrode is connected to ground, which makes the input voltage between working and reference electrodes vary from 0 V to -1.5 V and back to 0 V. Although the sweeping range could be -1.6V~+1.5V, positive potential is avoided in case of oxidation of the silver working electrode. Integrated operational amplifiers are used in circuit as potentiostat, and a trans-

impedance circuit is applied to convert the current to voltage. Since the frequency of this output voltage is low (below the detection limit of the mobile phone microphone) and the amplitude is higher than the detection limit of the microphone input, a frequency modulation (FM) module is added to the circuit to convert the sensing data to the signal with the allowed frequency range of the microphone jack. Besides the basic frequency modulation, frequency demodulation and potentiostat circuit, other circuit components like low pass filter, amplifier and voltage buffer were also used to transfer signal between separate stages. A detailed circuit diagram is in Figure 3.3.

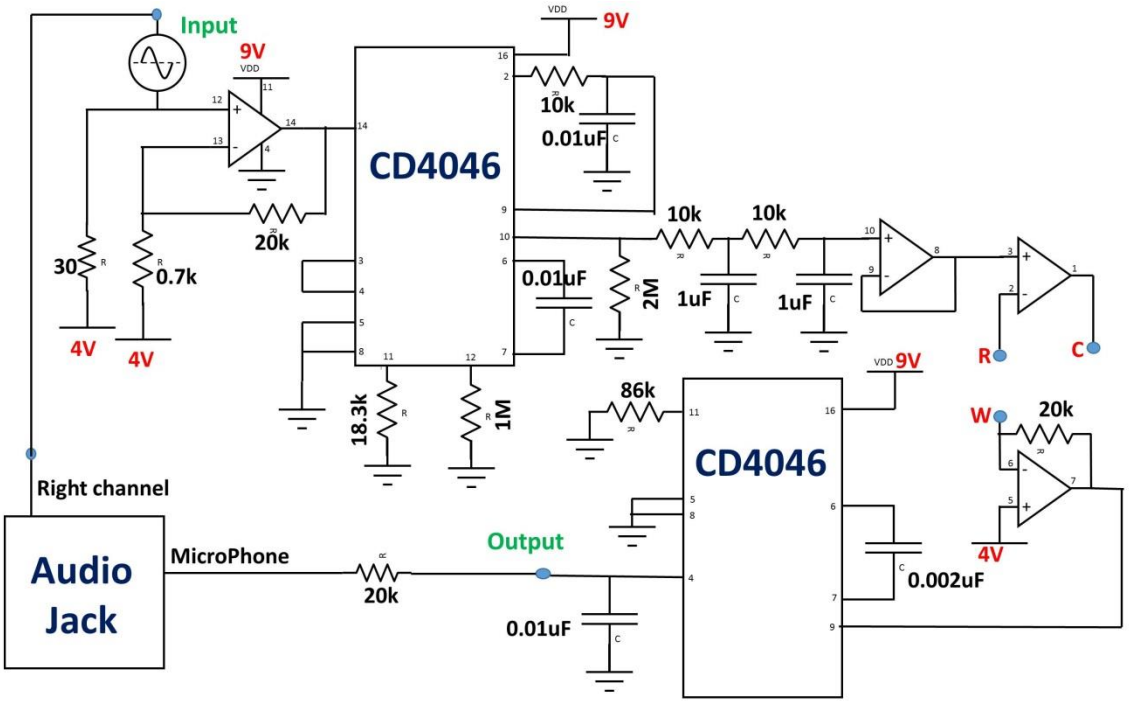

Figure 3.3 Circuit diagram in detail for MoboSens system, including the circuit for frequency modulation and demodulation, as well as the circuit for achieving potentiostat.

3.4 Smart phone data processing

Since the raw data recorded by the mobile phone platform is a series of square waves at different frequencies from the FM integrated circuit (CD4046), averaging of frequency data over a window is performed to obtain the raw data. The FM property of CD4046 is first characterized. Then a calibration method is employed to transform the frequency values to voltage values. The sampling rate of the smart phone is 32000 bytes/s and each voltage value is stored as a short integer, so 16000 data are recorded each second. The output from the CD4046 is a square wave with amplitude larger than 0.7 V, but the input/output to the microphone inside a Windows phone is limited to 200 mV (this value will differ for different brands of phone). Hence, the recorded wave is a truncated square wave with maximum and minimum values of + 32767 (215 for signed short integer with 16 bits) respectively. The frequency value is calculated by counting the number of steps from maximum to minimum by setting 1600 samples as one period. Calibration is performed to convert the output frequency from the frequency modulation integrated circuit into voltage and finally to oxidation-reduction current using trans-impedance circuit. Based on the frequency modulation module, the relation between current and frequency is as follows:

$$\text{Current(A)} = (\text{frequency(kHz)} * 0.5627 + 0.3552 - 4.1)\text{(V)}/\text{resistor}(\Omega) \qquad (3.1)$$

3.5 Smart phone application interface

The software operates on a Samsung mobile phone with Windows Phone 7.5 OS (Android and iOS applications have also been developed; here, as an example, we describe Windows-based applications). The structure of the software application is provided in Figure 3.4. There are three layers from low to high, which are the basic functions provided by Microsoft, sensor API (Application Programming Interface) and user interface. The sensor API is the core of this

platform, which packages functions provided by Microsoft and is called by users' commands. In the user interface, there are four basic functions: start, sensing, display and stop. The start function enables the sweeping voltage to drive the nitrate sensor; it also provides a library of waveforms. The sensing function is mainly used to retrieve data from the output of the nitrate sensor, and to analyze data including FM demodulation, down sampling and calibration. The display function is used for plotting the results for visualization. The stop function can be used for terminating these functions during operation.

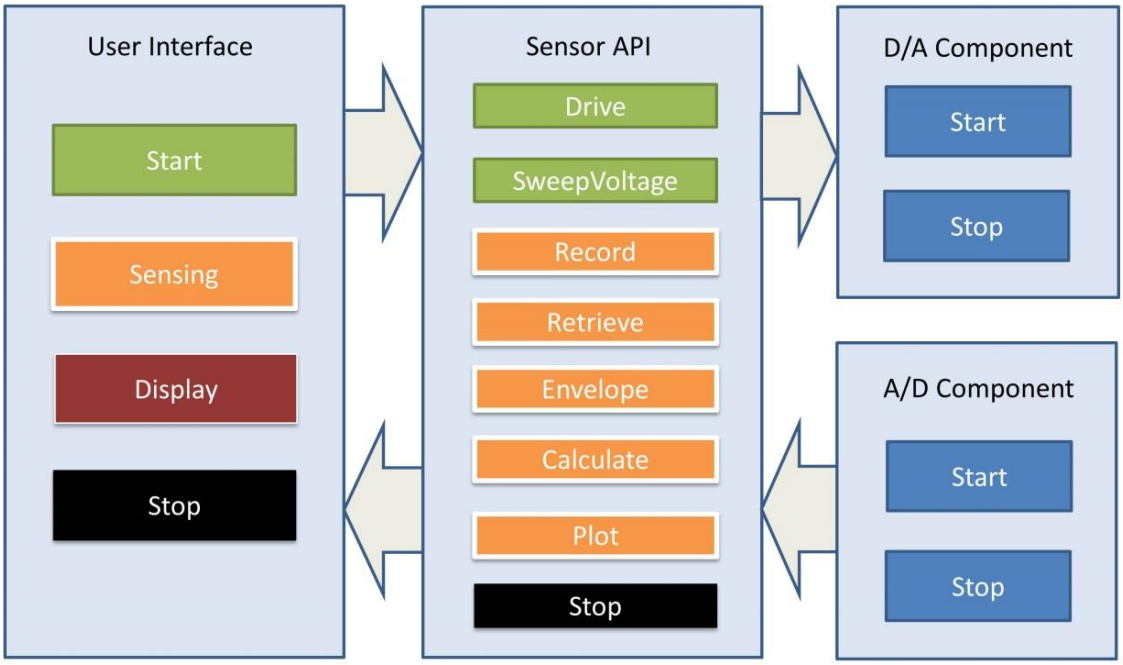

Figure 3.4 User interface and API structure. Four functions will be shown to users in the user interface while API functions in the lower level are well defined to be called by the basic four functions. D/A (play) and A/D (record) functions are called by API functions whenever signal transmission is needed through the audio jack.

The application on the Windows phone is further developed to integrate the location of testing (longitude and latitude) to the nitrate sensing and to display it on Bing maps. The temperature

data is also included in the nitrate sensing. The phone application also enables users to add any metadata (such as user comments and graphics) along with the shared nitrate sensing information provided by the user. The user has the option to send this sensing data to social networks such as Twitter for public dissemination or upload to a secure cloud server for further analysis. An example of the developed phone application interface is given in Figure 3.5. Figure 3.5 (a) shows the main page of the application. Figure 3.5 (b) displays a plot from a testing result. Through the interface showing in Figure 3.5 (c), users will be able to send metadata along with the testing results. Figure 3.5 (d) shows the location of the performed test on a Bing Map. After metadata is sent to Twitter, a message about nitrate information can be seen posted on the network, as shown in Figure 3.5 (e). Figure 3.5 (f) shows the satellite view of the location where testing is performed with nitrate information labeled.

Figure 3.5 User interface and network connection of MoboSens app. **(a)** Front page of the app. **(b)** Testing results plotted on the phone screen. **(c)** Interface showing the ability to input user "metadata", along with the ability to pull publicly available data (e.g., USGS weather data) and showing them in one map. **(d)** Bing map interface with the current location of the experiment shown on the map. **(e)** Message posted on Twitter through the MoboSens platform. **(f)** Satellite view of recently posted data.

CHAPTER 4

SMART PHONE BASED NITRATE SENSOR FOR REAL APPLICATION

4.1 Overview

Here we presented a lab-on-a-chip mobile sensing system (MoboSens), which includes a miniaturized electrochemical sensor, mobile phone platform (mobile phone application and controlling circuit) to control the sensor and microfluidics to handle the liquid samples. The use of miniaturized electrodes has several advantages such as low ohmic drop, low capacitive current, small time constant and fast mass transport [18, 19]. A user-friendly mobile application interface is developed which enables a simple and easy-to-use testing procedure. Due to its lightweight (~65 gram) and small form factor, the whole system is portable. Unlike some smart phone based sensing platforms developed previously [26, 27], our platform makes use of the audio jack as the sensing interface instead of the camera. The embedded camera on a smart phone enables people to do image or spectrum analysis in the mobile application [31, 32, 33, 34], but the application is limited only to "retrieving" signal. Using the audio jack can break through this one-way communication by setting a mechanism which will both "send" and "retrieve" signals, just as is done when people listen to music and record a voice. The use of micro USB interface to perform electrochemical testing was done previously, but without achieving cross-platform testing easily because of the different protocols for different smart phones like Samsung (Android system) and iPhone (iOS system) [35]. In addition, the audio jack has been used to generate a voltage excitation signal for electrochemiluminescence detection [36]. However, it suffers from cross-platform incompatibility since the voltage value generated from the audio jack varies among

different phones. Instead, what we generated and received from the audio jack is not the sound volume but the tone frequency, which can break through this cross-platform limitation. This enables us to do different electrochemical testing by generating smooth waveforms. Recently, the audio jack was also used to send a control signal from the phone to an external integrated potentiostat to perform different electrochemical tests [37]. In contrast, by making use of the CPU, ADC and DAC from phone itself, instead of external electronic components, we are able to minimize the form factor and cost (~ $10) of our package to achieve one hand-held platform to do electrochemical testing. Currently, the smart phone based system is designed for nitrate concentration measurement. Further development of the sensor is underway to include detection of other ions like phosphate or microbial contaminants like bacteria [38].

4.2 System characterization and field testing

Sodium nitrate solutions at different concentrations (100 μM (1.4 ppm NO3-N) to 5 mM (70 ppm NO3-N)) with 0.1 M NaOH electrolyte medium were tested by the MoboSens platform. Figure 4.1 (a) shows the recorded frequency changing with sweeping voltage. The frequency values were converted to voltage first, by using the linear voltage-to-frequency relationship shown in Figure 4.2 (b). The current values were then calculated by dividing the resistance value of the resistor where the current passes through as shown in Figure 4.1 (c). During the forward sweeping process (0 V to -1.5 V), there are current peaks which occur at around -1.35 V ~ -1.4 V. The magnitude of the reduction current peaks is dependent on the concentration of nitrate present in the solution. The position of the reduction peak shifts about 50 mV to more negative value as the concentration of nitrate increases. This shift could be due to the existence of uncompensated resistance (R_u). Unlike a commercial potentiostat, which has a good control of $E + iR_u$ between working and reference electrodes (E is the potential applied to working electrode), we controlled

the true potential applied on the working electrode. The practical effect of uncompensated resistance is to shift the reduction peak toward more negative potentials, especially in higher scan rate and higher concentration conditions which cause larger reduction current [19]. The small wide peaks around -0.9 V could be attributed to hydroxide desorption on the silver electrode [15, 39]. In the anodic sweeping process, an anodic current peak occurs at around -1.25 V, which is due to the electro-chemisorption of hydroxide ions [28, 39].

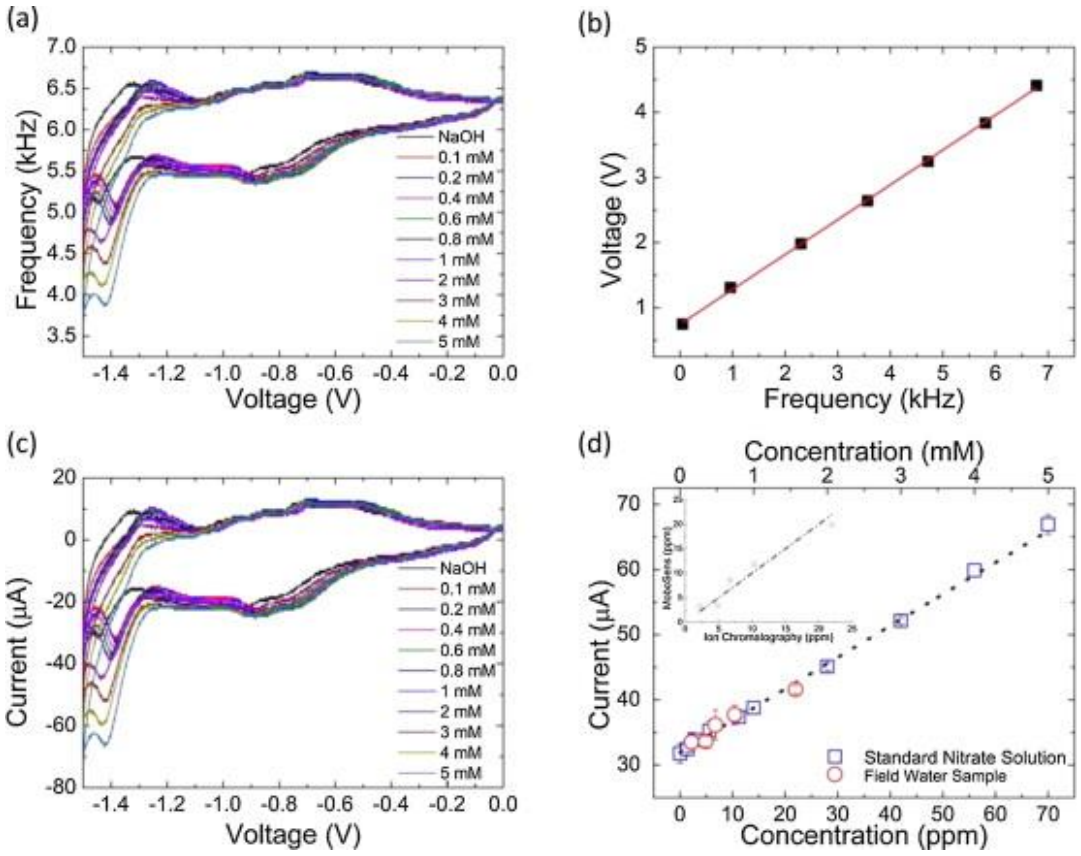

Figure 4.1 Measuring nitrate using MoboSens. **(a)** Raw data from MoboSens platform as frequency values. **(b)** Calibration curve of CD4046 to convert frequency values to voltage. **(c)** Cyclic voltammetry testing of standard nitrate solution at 0.1 ~ 5 mM (1.4 ~ 70 ppm NO3-N) using MoboSens platform at a scan rate of 100 mV/s. **(d)** Measurement of nitrate concentration in field water sample using MoboSens platform. For comparison, the field sample data are shown directly on the calibration curve obtained from standard nitrate solution shown in (c). Inset of (d) is the MoboSens deviation from ion chromatography data by fitting experimental data into calibration curve. The electrolyte (NaOH) concentration is 100 mM**.**

The calibration curve is obtained from the current reduction peak values after data processing in Figure 4.1 (d). With linear fitting method, calibration equation could be written as:

$$\text{Current(A)} = -4.8506 \times 10^{-7}\text{Concentration(ppm)} - 4.3973 \times 10^{-5} \quad (4.1)$$

The relation between reduction current and concentration shows linearity within the concentration range in 100 μM (1.4 ppm NO3-N) ~ 5 mM (70 ppm NO3-N). The blue data points in Figure 4.1 (d) are measurement from standard nitrate solution while red data points are measurement from field water samples provided by Department of Agriculture at the University of Illinois. The statistical error bar is based on four testing results using the same concentration. For the standard nitrate solution, samples with low concentration (~2 ppm) show larger standard deviation compared with samples having higher concentration of nitrate. Since there is always oxygen dissolved in solution, the deviation from linearity could be due to oxygen reduction. This reaction interferes with nitrate measurement by taking place at a more positive potential than nitrate reduction [15, 24]. We anticipate this effect will be more pronounced at lower concentration of nitrate (< 2 ppm), and hence, will not challenge the reliability of the sensor to measure nitrate at higher concentration (> 2 ppm).

The field water samples are first filtered using a 0.1 μm Whatman filter paper to remove the suspended particles. For comparison, the concentrations of nitrogen in nitrate were measured by Dionex ion chromatography with a detection limit of 0.08 ppm. Figure 4.1 (d) shows nitrate concentration of field water samples (red circle) measured by MoboSens platform and compared with the calibration curve obtained with nitrate standard solution (blue square). The inset of Figure 4.1 (d) shows the comparison of MoboSens results with those of ion chromatography measurement for the same field water samples. The measurements are within + 15% deviation at

low concentration (2.2 ppm) and + 5% deviation at high concentration (22 ppm). This verifies the ability of the MoboSens platform to perform farm-based field water testing.

4.3 Limit of detection for environmental water

In addition to the field water sample, MoboSens was utilized to measure nitrate concentration in environmental water samples. By adjusting the trans-impedance from 20 kΩ to 100 kΩ, the detection limit could be pushed to more diluted nitrate solution (around 10 μM (0.14 ppm)). The principle of trans-impedance is to convert current to voltage and voltage is converted to frequency as mentioned earlier. This adjustment is to fit a lower concentration range into a wide frequency range. Figure 4.2 (a) shows the results of standard nitrate solution with low concentration (less than 1.4 ppm). The reduction current peaks are calibrated in Figure 4.2 (b). Testing was then performed for environmental water samples. These water samples were collected from different sources like lakes, streams and local wells. The raw data was processed with the method described in the previous section and the peak current was fitted into the calibration equation. To verify the accuracy of measurement results obtained using this mobile sensor platform, methods like cadmium reduction and ultraviolet (UV) absorption spectroscopy were performed for comparison [24]. The cadmium reduction method was based on the reduction of nitrate to nitrite on cadmium as a catalyst, followed by Griess reaction to form a fluorescent chemical. Cadmium reduction method is normally considered the “gold standard” for the detection of nitrate level. The UV absorption spectroscopy method was performed by scanning wavelength in a range from 190 nm to 450 nm. Nitrate concentration was calibrated from the absorption spectrum at different concentrations. The comparison of nitrate concentration of different water samples after calibration using the three different methods is shown in Figure 4.2 (b).

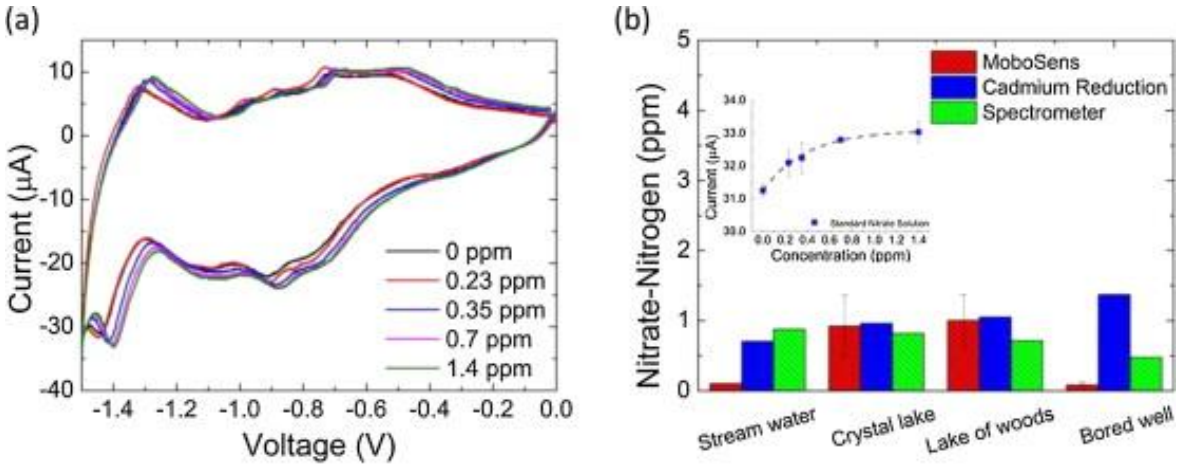

Figure 4.2 Limit of detection of MoboSens platform. **(a)** Cyclic voltammetry testing for standard nitrate solution at sub-ppm concentration using MoboSens platform at a scan rate of 100 mV/s. **(b)** Comparison of different analytical methods to measure nitrate concentration in environmental water sample. The electrolyte (NaOH) concentration is 100 mM.

From the results, the coefficient of variation (COV) of nitrate concentration in Crystal Lake and Lake of the Woods, Illinois, with respect to cadmium reduction method is 4.1% and 4.7% respectively. The concentration of nitrate ion tested by MoboSens from these two water sources is consistent with the cadmium reduction method. Water from streams and bored well shows much lower concentration in MoboSens compared to other methods, especially a large COV with respect to the cadmium method. The large COV is attributed to the presence of nitrite in the sample as cadmium reduction methods convert nitrite into nitrate first and then measure the total nitrogen. Above all, the nitrate concentrations of all water samples were far below 10 ppm, which satisfied the requirements for water safety prescribed by the EPA.

CHAPTER 5

CONCLUSION

In summary, we have demonstrated an audio jack-based mobile sensing system for rapid and real-time nitrate concentration measurement. It contains a micro-fabricated three-electrode sensor, a mobile application and a circuit board developed for communicating with the sensor. The mobile sensing platform was used to test nitrate ion levels in field water as well as environmental water samples and compared with existing analytical testing methods. The mobile platform sensing was found to be comparable with the traditional sensing methodology. Finally, the measured concentration value, location of testing site and metadata such as user inputs are communicated and shared on social networks and on a secured cloud server for further analysis.

REFERENCES

[1] K. Fajerwerg, V. Ynam, B. Chaudret, V. Garcon, D. Thouron, M. Comtat, *Electrochemistry Communications* **2010**, 12, 1439-1441.

[2] Environmental Protection Agency, List of contaminants & their maximum contaminant level (MCLs). *http://www.epa.gov/safewater/contaminants/dw_contamfs/nitrates.html*.

[3] M.J. Moorcroft, J. Davis, R.G Compton, *Talanta* **2001**, 54, 785-803.

[4] A. Buldt, U. Karst, *Anal. Chem.* **1999**, 71, 3003-3007.

[5] D.L. Granger, R.R. Taintor, K.S. Boockvar, J.B. Hibbs, *Methods In Enzymology* **1996**, 268, 142-151.

[6] B. Hemmens, B. Mayer, *Methods in Molecular Biology*, **1997**, 100, 1-32.

[7] H. Wang, W. Yang, S. Liang, Z. Zhang, H. Zhang, *Analytica Chimica Acta,* **2000**, 419, 169-173.

[8] S. Kage, K. Kudo, N. Ikeda, *J. Chromatography* **2000**, 742, 363-368.

[9] M.I.H. Helaleh, T. Korenage, *J. Chromatography* **2000**, 744, 433-437.

[10] M.J. Dunphy, D.D. Goble, D.J. Smith, *Analytical Biochemistry* **1990**, 184, 381-387.

[11] H. Kodamatani, S. Yamazaki, K. Saito, T. Tomiyasu, Y. Komatsu, *J. Chromatography A* **2009**, 1216, 3163-3167.

[12] G.M. Janini, K.C. Chan, G.M. Muschik, H.J. Issaq, *J. Chromatography* **1994**, 657, 419-423.

[13] A.A. Okemgbo, H.H. Hill, W.F. Siems, *Anal. Chem.* **1999**, 71, 2725-2731.

[14] G. Hanrahan, D.G. Patil, J. Wang, *J. Environ. Monit.* **2004**, 6, 657-664.

[15] D. Kim, I.B. Goldberg, J.W. Judy, *Analyst* **2007**, 132, 350-357.

[16] M.A. Bhat, P.P. Ingole, V.R. Chaudhari, S.K. Haram, *New J. Chem.* **2009**, 33, 207-210.

[17] S. Li, J. Kiehne, L.I. Sinoway, C.E. Cameron, T. J. Wang, *Lab Chip*, **2013**, 13, 3993-4003.

[18] D. Kim, I.B. Goldberg, J.W. Judy, *Sensors and Actuators B: Chemical* **2009**, 135, 618-624.

[19] A.J. Bard, L.R. Faulkner, *Electrochemical Methods: Fundamentals and Applications*, second ed., Wiley, **2000**.

[20] S. Cattarin, *J. Appl. Electrochem.* **1992**, 22, 1077-1081.

[21] M. Fedurco, P. Kedzierzawski, J. Augustynski, *J. Electrochem. Soc.* **1999**, 146, 2569-2572.

[22] G.E. Dima, A.C.A. de Vooys, M.T.M. Koper, *Journal of Electroanalytical Chemistry* **2003**, 554-555, 15-23.

[23] M.R. Majidi, K. Asadpour-Zeynali, B. Hafezi, *Int. J. Electrochem. Sci.* **2011**, 6, 162-170.

[24] M.R. Gartia, B. Braunschweig, T.W. Chang, P. Moinzadeh, B.S. Minsker, G. Agha, A. Wieckowski, L. L. Keefer, and G.L. Liu, *J. Environ. Monit* **2012**, Advance Article.

[25] J. Krista, M. Kopanica, L. Novotny, *Electoanalysis* **2000**, 12, No. 3, 960-962.

[26] S.K. Vashist, O. Mudanyali, E.M. Schneider, R. Zengerle, A. Ozcan, *Anal Bioanal Chem*, **2014**, 406(14), 3263-3277.

[27] A. Ozcan, *Lab Chip*, **2014**, 14, 3187.

[28] E.R. Savinova, P. Kraft, B. Pettinger and K. Doblhofer, *J. Electroanal Chem.* **1997**, 430, 47-56.

[29] R. Zadro, B. Pokric, Z. Pucar, *Analytical Biochemistry* **1981**, 117, 238-244.

[30] Soil Survey Division Staff. **1993**. Soil Survey Manual. United States Department of Agriculture Handbook N0. 18. Washington, DC. 437 pp.

[31] D. Gallegos, K.D. Long, H. Yu, P.P. Clark, Y. Lin, S. George, P. Nath, B.T. Cunningham, *Lab Chip*, **2013**, 13, 2124.

[32] Q. Wei, R. Nagi, K. Sadeghi, S. Feng, E. Yan, S.J. Ki, R. Caire, D. Tseng, A. Ozcan, *ACS Nano*, **2014**, 8(2), 1121-1129.

[33] S.K.J. Ludwig, H. Zhu, S. Phillips, A. Shiledar, S. Feng, D. Tseng, L.A. Ginkel, M.W.F. Nielen, A. Ozcan, Anal Bioanal Chem, **2014**. DOI: 10.1007/s00216-014-7984-4

[34] Q. Wei, H. Qi, W. Luo, D. Tseng, S.J. Ki, Z. Wang, Z. Gorocs, L.A. Bentolila, T. Wu, R. Sun, A. Ozcan, *ACS Nano*, **2013**, 7(10), 9147-9155.

[35] P.B. Lillehoj, M. Huang, N. Truong and C. Ho, *Lab Chip*, **2013**, 13, 2950-2955.

[36] J.L. Delaney, E.H. Doeven, A.J. Harsant, C.F. Hogan*, Analytica Chimica Acta*, **2013**, 790, 56-60.

[37] A. Nemiroski, D.C. Christodouleas, J.W. Hennek, A.A. Kumar, E.J. Maxwell, M.T. Fernández-Abedul and G.M. Whitesides, *PNAS*, **2014**, 111(33), 11984-11989.

[38] J. Jiang*, X. Wang*, R. Chao, Y. Ren, C. Hu, Z. Xu and G. L. Liu, *Sensors and Actuators B: Chemical*, **2014**, 193, 653-659.

[39] E.R. Savinova, S. Wasle, K. Doblhofer, *J. Electrochim. Acta* **1998**, 44, 1341-1348.